Small Scale Crater Detection Based on Deep Learning with Multi-temporal Samples of High-resolution Images

Yanmin Jin, Fan He, Shijie Liu, Xiaohua Tong
College of Surveying and Geo-Informatics
Tongji University
Shanghai, China
jinyanmin@tongji.edu.cn, liusjtj@tongji.edu.cn

***Abstract*—This paper presents an automated method for small-scale crater detection from high resolution images based on deep neural network. And the network performance is improved by the use of a multi-temporal samples extraction technique. Obtaining topographical features of planet surface, such as craters, is of great importance. It contributes to the understanding of planetary geology. And the detected craters serve as important research objects during the whole aerospace engineering process like landing and navigation of rovers. The large scale craters detection have been extensively studied. However, with the development of high resolution sensors of Moon and Mars, methods specified on extracting smaller craters from high resolution image (HRI) are needed. But dealing with HRI is tricky because: (1) small ground targets can be varied largely in images of different illuminations; (2) A small crater's shape could easily erode over time to blend into the surface; (3) The number of the small craters are much larger than that of the large carters. These problems are properly addressed in this paper using the proposed method. Experiments with the images of the Chang'e-4 landing area proved that this method is practical and has an accuracy of 92.9% which is higher than other methods.**

Keywords—crater detection, multi-temporal, deep learning, samples extraction

I. INTRODUCTION

The craters on planets are potential terrain hazards for high-precision spacecraft landing and rover navigation missions [1-3]. Therefore, it is of great importance to extract the craters accurately.

Much research attention has been paid to the crater extraction. Traditionally, the extraction of craters from planet surface images was mainly carried out by visual inspection [4]. B Leroy and E Johnson [5] proposed a ellipse detection method based on the generalized Hough transform (GHT) to identify asteroid impact craters. C. Yang et al. [6] combined the illumination direction with the crater edge information to achieve the extraction of craters. In recent years, machine learning algorithms has become popular. Tomasz. F Stepinski [7] used the support vector machine method to classify craters and reached an accuracy of 91%. Joseph. P Cohen et al. [8] applied deep neural networks to classify the original image as crater and non-crater regions and achieved an accuracy of 88.78%.

Studies mentioned above mainly focus on large scale craters detection, while small-scale craters are also important for engineering purpose. But as to extraction of small scale craters, three problems become critical: (1) One ground target can be varied significantly in different images (Fig. 1). Terrain relief, illumination condition, camera attitude, etc., will all greatly affect craters' appearances. (2) A crater could easily be eroded over time and even be blended into the surface [9]. This problem is more crucial for small scale craters because they are more susceptible to wind factor and geologic factor. (3) The magnitude of craters increases exponentially as the decrease of crater size. D. De Rosa et al. [10] has proved this with manual crater extraction from images.

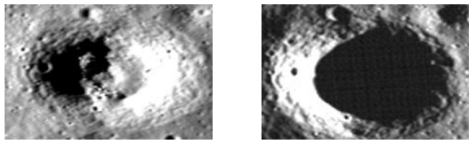

Fig. 1. The same crater in images with different illumination conditions.

To address the problems mentioned above, this paper introduced a crater detection procedure using the state-of-art deep neural network Faster R-CNN(Faster region convolutional neural network) which performs well at complicated targets due to its multiple convolutional layers and proposal box regression. In order to handle the complicated sample selection and extraction problem in high resolution images, this paper also proposed a new method to acquire better training samples by using multi-temporal images. The full procedure will be introduced in section II and experiments in section III.

II. METHODS

A. Multi-temporal Training Samples Extraction

There are two features that distinguish crater detection from other detection tasks. First, the images used in crater detection are subjected to rigorous photogrammetry geometric relations. Therefore, they are geocoded with geographic coordinates which is an advantage comparing to regular pictures. Second,

there is lack of authenticity verification for outer space craters. Therefore, there is higher demand on the accuracy of sample selection than the targets on the earth. To accommodate those characteristics, we utilize multi-temporal images to perform automatic sample matching and get multiple samples from craters. The contributions of this method are:

- **Increased model robustness to illumination conditions.** One crater under different illumination conditions can be put into the training machine altogether since this crater is geocoded with same coordinates in different images.
- **Increased sample pool size while reducing repetitive work.** With multi-temporal images, a large number of training samples can be acquired at the same time, reducing the amount of labor.
- **Reduced the error rate of manual sample selection.** once a sample crater is selected in one image, other samples in the same group are selected synchronously, Reducing the possibilities of losing positive samples.

The proposed method is performed in the following steps:

1) Image splitting and grouping: The multi-temporal images are splitted into small pieces (e.g. 1000*1000 pixels). The size of the splitted piece depends on the minimum size of crater that need to be detected. Then the splitted images are grouped according to the center coordinates of each image, ensuring that images in one group have the same geographical location, and different imaging time.

2) Image registration: Although theoretically, images within a group should be geographically corresponding, the overall offset and small distortions of each image piece are still possible, which would cause errors in automatic sample matching. Therefore, the Scale-invariant feature transform (SIFT) algorithm [11] is used to perform registration within the group. After registration, the non-public parts are clipped off to acquire strictly corresponding multi-temporal image groups.

3) Sample extraction: Inside each image group, manual sample extraction is performed for each image. Each extracted sample generates several samples along with it(e.g. a group with 5 multi-temporal images generate 5 samples). Fig. 2 shows how we get multiple training samples of one crater under different imaging conditions.

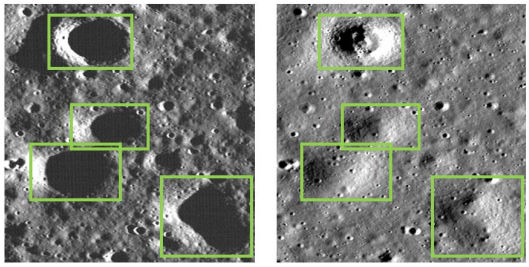

Fig. 2. Multi-temporal training samples: (a) crater samples manually selected by the operator. (b) crater samples automatically selected by image matching. 3 craters in the lower part of (b) are not obvious to human eyes.

B. Faster R-CNN Detection Algorithm and ResNet Model

In order to detect craters, traditional unsupervised methods use elliptical fitting or morphology, etc. [4]. Earlier machine learning methods also used artificial features, all of which are common on depending on domain knowledge to construct their algorithm [3]. However, in the case of high-resolution small-scale crater detection, many aspects will limit the performance of these methods, e.g. complex terrain relief and illumination conditions. Therefore, the state-of-the-art deep neural network detection algorithm is adopted.

Faster R-CNN is a target detection algorithm based on convolutional neural network (CNN) [12]. Firstly, the CNN generates the feature map from the input data, and the Region Proposal Network (RPN) determines a large number of suggestion boxes. Then one proposal's classification probability and its bounding box regression are trained iteratively until the model reaches its best performance.

The specific network structure we choose is ResNet101 (the model consists of 101 layers) [13], which is currently one of the best performing deep neural network model. ResNet (Fig.3) consists of multiple convolutional layers of different scales and anchors.

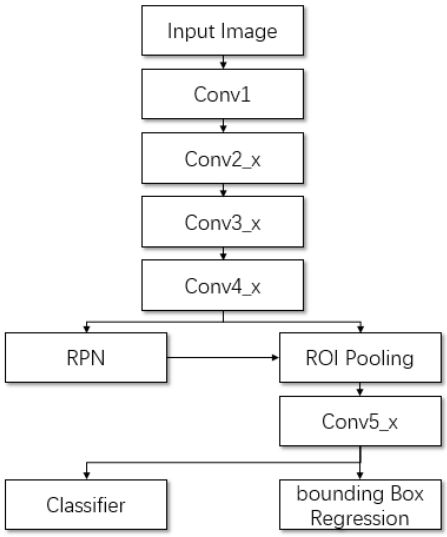

Fig. 3. A Simplified flow chart of using ResNet with Faster R-CNN detection model. (More detailed information about the construction of it can be found in [13])

III. EXPIRIMENTS

The proposed approach was used to detect craters from the narrow-angle camera of the lunar reconnaissance orbiter camera (LROC NAC) images acquired from NASA's Planetary Data System. The average resolution is 1.4m/pixel. The test area is near the Chang'e-4 landing site (177.588°E，45.457°S) inside the Von Kármán crater at South Pole Aitken basin. Furthermore, three images with different illumination conditions at different times in the area were selected.

A. Pre-processing of Images

Firstly, the acquired images are pre-processed with Integrated Software for Imagers and Spectrometers (ISIS), The

entire process includes format conversion, ephemeris acquisition, CCD image unit splicing, radiation correction, map projection. All these procedures were done in ISIS software with a small amount of manual operation. In addition, since the gray value of the acquired image is low in overall, the image appears to be dark. To improve the visual effect of the image and enhance the contrast of the image, we use the linear truncation method of the image gray scale:

$$\boldsymbol{c}(x,y)=\frac{d-c}{b-a}\times \boldsymbol{f}(x,y)+\frac{bc-ad}{b-a} \quad (1)$$

where *f(x, y), a ,b* are each pixel's gray value, minimum and maximum gray value of image before stretching, *c(x,y), c, d* are those after stretching. After the procedure, the brightness and contrast of the image are improved.

B. Training Samples Extraction

After acquired pre-processed images, we split them and sorted the pieces into 43 groups using the method in section II.A. In addition, we performed some artificial check on the matching process to avoid the error matching being brought into next step.

The image annotation tool LabelImg was used for sample extraction. LabelImg provides a graphical interface that allows operators to label samples and record them as an XML document. Furthermore, we improved this tool in our practice such that, once one sample is labeled, the same position of the set of images is synchronously labeled.

In this experiment, we aims to detect craters larger than 50 pixels(diameter of 75 meters) by considering the resolution of the image and the magnitude of craters,. Accordingly, only craters larger than 50 pixels are extracted as training samples.

C. Building and Training ResNet101

Neural network construction can be done using the TensorFlow library developed by Google. It provides a complete set of functions for network building and training.

The training samples were divided into three subsets, a training set, a verification set and a test set. The training set is used to calculate the weights of the neurons in the model. The validation set is used to determine the network structure and the parameters that control the complexity of the model, while the test set tests the performance of the final selected optimal model. Among the 43 groups of images, 23 groups (69 images, about 350 craters) were used as the test set, 10 groups (30 images, about 150 craters) as the verification set, 10 groups (30 images, about 150 craters) as the test set.

D. Results and Comparison

The training model was performed 70,000 iterations in the ResNet network, and the GPU computing (NVIDIA Quadro P2000) took 30 hours. The loss function of the model increased with the number of iterations and finally stabilized at around 0.14. Fig. 4 shows the model training process. We can see that the loss function has a downward trend. If we need to further save training time, we can shorten the iterations to 20,000 at the expense of the loss function increasing 0.06, and total time cost will be controlled within 5 hours.

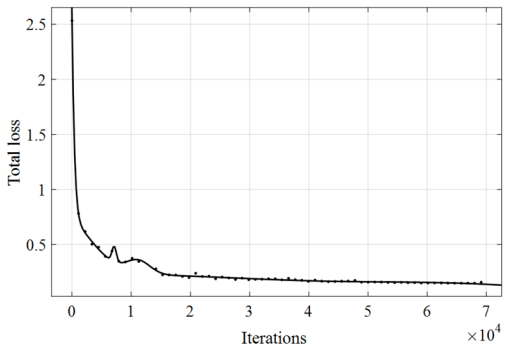

Fig. 4. The total loss function value of the model

In all the 10 test groups, a total of 142 craters were detected, of which 132 were correct craters, 10 were false detected, so the overall accuracy of the proposed method is 93.96%. Meanwhile, there are 148 craters in total, of which 132 were successfully detected, 16 were missing, so the recall rate is 89.19%. Two test images marked with craters detected by the trained model are shown in Fig. 5.

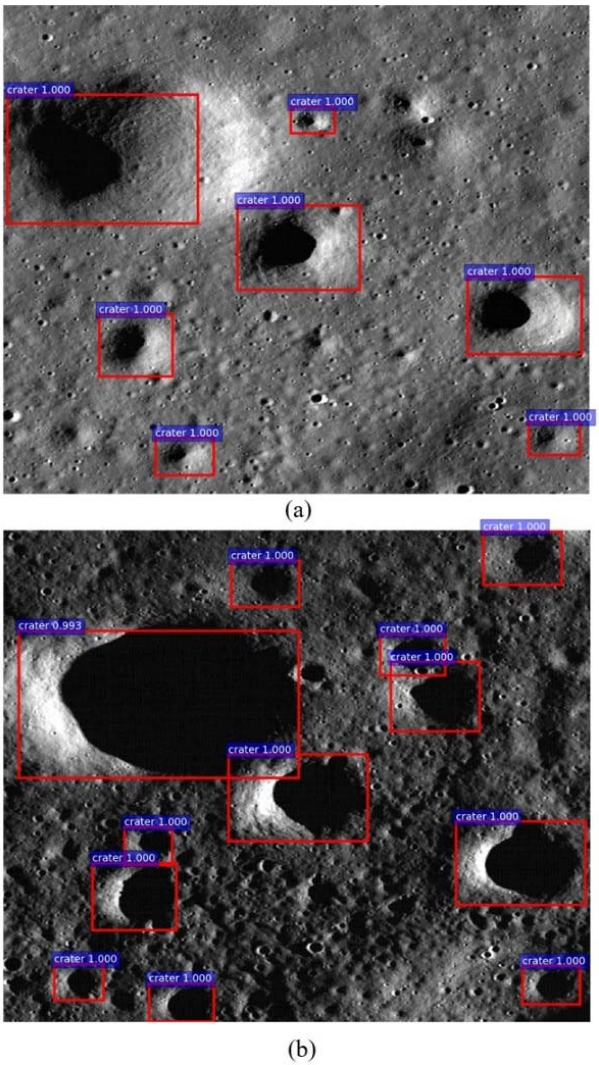

Fig. 5. (a) Test image that are marked with detected craters. (b) Another test image that are in the same group but with lower solar elevation angle.

In order to verify the contribution of the proposed multi-temporal sample extraction method, we set up another two samples sets, and put them into the same ResNet network to compare the outcomes. The dataset I used only one of the crater samples from each group of crater samples, so the total sample pool size is 1/3 (with the same amount of work in samples extraction); the dataset II also used only one of the crater samples from each group of the crater samples, but triple sample pool size by adding new crater samples (same amount of samples but triple workloads).

TABLE I. RESULTS OF TESTS

	Original dataset	***dataset I***	***dataset II***
Accuracy rate	92.96%	88.70%	91.60%
Recall rate	89.19%	68.92%	73.65%

The data in Table 1 shows that, (1) by comparing with I ,the multi-temporal training samples extraction method proposed in this paper effectively improves the detection accuracy and recall rate. (2) And by comparing with II, the detection accuracies are basically the same (because the same amount of training samples), but the recall rate is increased by 15%, besides, the workload of extracting samples is greatly reduced.

Furthermore, in order to compare the detection efficiency of the Faster R-CNN algorithm, we use the same training sample to perform another machine learning target detection algorithm which is Support Vector Machine (SVM) classifier with Histogram of Oriented Gradient (HOG) features. This method is firstly used in face detection by Navneet Dalal [14] and have been successfully used in many area including large scale crater detection. The test results are shown in Table 2.

TABLE II. RESULTS OF TESTS

	This method	***SVM classifier + HOG features***
Accuracy rate	92.96%	62.32%
Recall rate	89.19%	58.11%

The total training time is about 5 hours, but the detection time of each test image is about 2 seconds. From the results in Table 2, we can see that, the traditional machine learning method of artificially constructed features performs poorly in high resolution small scale crater detection, while the end-to-end training algorithm ResNet network performs better both in accuracy and recall rate.

IV. COCLUSIONS

This paper presents an automated method for small-scale crater detection from high resolution images based on the state-of-the-art deep neural network detection algorithm. To overcome several difficulties when extracting samples in high resolution images, this paper introduced a new sample extraction method with pre-processed multi-temporal images. And experiments of the LROC NAC images showed that (1) this Faster R-CNN detection algorithm is effective and out-perform traditional machine learning algorithms, (2) this multi-temporal sample extraction method significantly increases recall rate by about 15% while greatly reduces workload.

Future work will be focusing on making some internal changes to the ResNet structure and achieving a better result at recall rate. Moreover, more experiments of other areas and images are planned to perform, to acquired a complete craters database product.

ACKNOWLEDGMENT

The work described in this paper was substantially supported by the National Natural Science Foundation of China (Project No. 41601414), the Shanghai Sailing Program (Project No.16YF1412200) and Fundamental Research Funds for the Central Universities.

REFERENCES

[1] Yu, Z. , Zhu, S., Cui, P.: Sequence Detection of Planetary Surface Craters From DEM Data, World Congress on Intelligent Control and Automation, (2012)

[2] Maoyin A., Pan, W. : Crater Detection Algorithm With Part PHOG Features For Safe Landing, International Conference on Systems and Informatics, (2012) 103-106

[3] Emami E , Bebis G , Nefian A , et al. Automatic Crater Detection Using Convex Grouping and Convolutional Neural Networks[J]. 2015.

[4] Kamarudin N D , Ghani K A , Mustapha M , et al. An Overview of Crater Analyses, Tests and Various Methods of Crater Detection Algorithm[J]. Frontiers in Environmental Engineering, 2012, 1(1):7.

[5] B Leroy, G Medioni, E Johnson, et al. Crater Detection for Autonomous Landing on Asteroids [J] . Image and Vision Computer, 2001, 19(11) : 787-792.

[6] Yang C, Johnson A E, Matthies L H, et al. Optical landmark detection for spacecraft navigation[C]//Proceedings of the 13th Annual AAS/AIAA Space Flight Mechanics Meeting. 2003:1785-1803.

[7] Tomasz F Stepinski, Soumya Ghosh, Ricardo Vilalta. Machine Learning for Automatic Mapping of Planetary Surface [C]// Proceedings of the 19th National Conference on Innovative Applications of Artificial Intelligence. AAAI Press, 2007: 1807-1812.

[8] Cohen J P, Lo H Z, Lu T, et al. Crater detection via convolutional neural networks[J]. arXiv preprint arXiv:1601. 00978, 2016.

[9] L. Bandeira, W. Ding, and T. F. Stepinski, "Automatic Detection of Sub-km Craters Using Shape and Texture Information," in Proceedings of the 41st Lunar and Planetary Science Conference, Mar. 2010.

[10] De Rosa, D. , et al. "Characterisation of Potential Landing Sites for the European Space Agency's Lunar Lander Project." Planetary & Space Science 74.1(2012):224-246.

[11] Lowe D G. Object recognition from local scale-invariant features[C]// Iccv. 1999.

[12] Ren S , He K , Girshick R , et al. Faster R-CNN: Towards Real-Time Object Detection with Region Proposal Networks[J]. 2015.

[13] He K , Zhang X , Ren S , et al. Deep Residual Learning for Image Recognition[J]. 2015.

[14] Dalal N, Triggs B. Histograms of oriented gradients for human detection[C]//Computer Vision and Pattern Recognition, 2005. CVPR 2005. IEEE Computer Society Conference on. IEEE, 2005, 1: 886-893.